

Seed Laser Chirping for Enhanced Backward Raman Amplification in Plasmas

Z. Toroker, V. M. Malkin, and N. J. Fisch

Department of Astrophysical Sciences, Princeton University, Princeton, New Jersey 08544, USA

(Received 5 April 2012; published 22 August 2012)

Backward Raman compression in plasma enables pulse compression to intensities not available using material gratings. Mediating the compression with higher density plasma generally produces shorter and therefore more intense output pulses. However, very high density plasma, even if sufficiently tenuous to be transparent to the laser, also produces group velocity dispersion of the amplified pulse, deleteriously affecting the interaction. What is shown here is that, by chirping the seed pulse, the group velocity dispersion may in fact be used advantageously, achieving the maximum intensities over the shortest distances while minimizing unwanted effects.

DOI: [10.1103/PhysRevLett.109.085003](https://doi.org/10.1103/PhysRevLett.109.085003)

PACS numbers: 52.38.Bv, 42.65.Yj, 52.35.Mw

The largest laser intensities to date are achieved through the technique of chirped pulse amplification, which employs complementary gratings to stretch and then, after amplification, to re-compress light [1]. However, for picosecond pulses of wavelengths on the order of a micron, conventional materials cannot withstand laser fluences of more than several J/cm^2 , which limits intensities to several TW/cm^2 . For a vacuum focus beyond the grating of approximately 10^{10} , the current limit of intensities of about $10^{22} W/cm^2$ is reached. While there are plans for greater intensities through tighter focusing or larger gratings, to achieve the next generation of laser intensities, say by a factor of 10^3 , conventional material gratings or other focusing elements will likely have to be replaced by plasma.

In a plasma, a short counter-propagating seed pulse of frequency (ω_b), downshifted from a much longer pump pulse (of frequency ω_a) by the plasma frequency ω_e , can absorb the pump energy through a resonant three-wave interaction. This resonant backward Raman amplification (BRA) in plasma [2–4] in fact holds the promise of the next generation of intensities of exawatt and even zetawatt powers in reasonably compact facilities [5–13]. Moreover, by including chirped pulse amplification, together with Raman compression, the advantages of both schemes can be realized together for the highest intensity applications [14].

The Raman compression effect occurs because, in the nonlinear regime of pump depletion, the front of the seed pulse is amplified to the point of depleting the pump in a distance inversely proportional to the seed amplitude, shadowing any seed energy beyond that distance. As the seed grows, this length contracts, resulting in a self-similar self-contracting seed pulse regime for amplification [2]. The output pulses are limited by the bandwidth of the input seed pulses, and therefore, to achieve the shortest and therefore most intense output pulses, short seed pulses are necessary [2,15]. The output pulses are also limited in duration by approximately the plasma period $2\pi/\omega_e$ [2]. Because $\omega_e \sim n_e^{1/2}$, where n_e is the electron density, to

achieve shorter output pulses, denser plasma should be used. As the energy efficiency of this decay is proportional to ω_b/ω_a , it is inefficient to use the high density plasma except near the output stage, when the pulse is short. Thus, a two-stage process has been suggested wherein the output of the first stage serves as the pump for the second stage, where the higher density plasma is used, but only where it is needed most [16].

A further advantage to using higher density plasma, or what we might call *moderately undercritical* plasma, is that the phase velocity of the Langmuir wave, ω_e/k_f , is higher for a given seed or pump frequency [17]. The large phase velocity means that the Langmuir wave is less susceptible to Landau damping (allowing higher electron temperatures) as well as less susceptible to wave breaking (allowing higher pump intensities). Landau damping occurs when ω_e/k_f becomes comparable to the thermal velocity, $v_T = \sqrt{T_e/m_e}$. Wave breaking occurs when the trapping width equals the plasma wave phase velocity. Avoiding these damping mechanisms considerably broadens the parameter window over which Raman amplification can occur, which tends to narrow for short wavelength light [18,19].

However, at high density, the seed pulse undergoes significant group velocity dispersion, limiting the effectiveness of this method [17]. What we show here is that, by chirping the seed pulse, the group velocity dispersion may actually be advantageous. The chirping of the seed pulse is such that the front of the seed pulse, being at lower frequency, moves at a slower group velocity than does the rear of the seed pulse which is at higher frequency. If the chirp is matched to the group velocity dispersion, so that in the absence of the pump the pulse would be at a minimum duration upon exiting the plasma, the length to reach the highest intensity is considerably reduced. The fact that the plasma length is reduced has considerable advantages: first, there is less distance over which deleterious instabilities can develop, such as forward Raman amplification; second, there is less radiative loss through inverse

bremsstrahlung; and, third, less plasma is needed in the first place, requiring less energy.

In this Letter, we show first how chirping reduces the necessary plasma length in dense plasma. Then we show why chirping may be expected to produce this result—and why it should be optimal for minimum seed duration at the exit. First, to demonstrate the chirping effect, we solve the resonant three-wave equations in cold plasma, in the presence of both group velocity dispersion and relativistic nonlinearity of the amplified pulse. These equations may be put in the form [20]:

$$\begin{aligned} a_t + a_z &= bf, & f_t &= -ab^*, \\ b_t - b_z c_b/c_a &= -af^* - i\kappa b_{tt} + iR|b|^2 b. \end{aligned} \quad (1)$$

Here a , b , and f are envelopes of the pump, seed, and Langmuir waves, respectively, normalized such that the input pump amplitude is $a_0 = 1$. For such a normalization, the envelopes of electron quiver velocities in fields a , b , and f are caA , $cbA\sqrt{\omega_a/\omega_b}$, and $cfA\sqrt{\omega_a/\omega_e}$, respectively. Here ω_a , ω_b , and ω_e satisfy the resonance condition $\omega_a = \omega_b + \omega_e$, while A is the dimensionless vector potential of the input pump pulse, linked to the input pump intensity I_0 in plasma by the formula $A = \sqrt{2I_0\lambda_a/\omega_a e/m_e c^2}$, where λ_a is the pump wavelength in plasma, m_e is the electron mass, $-e$ is the electron charge, c is the speed of light in vacuum, and $\omega_e = \sqrt{4\pi n_e e^2/m_e}$ is the plasma frequency. The group velocities of the pump and seed laser pulses in plasma are $c_a = c\sqrt{1 - \omega_e^2/\omega_a^2}$ and $c_b = c\sqrt{1 - \omega_e^2/\omega_b^2}$. The time t is measured in units of $1/V_3 A$ and the distance z in units of $c_a/V_3 A$, where $V_3 = (k_f c/2)\sqrt{\omega_e/2\omega_b}$ is the three-wave coupling constant, $k_f = k_a + k_b$ is the resonant Langmuir wave number, $k_a = 2\pi/\lambda_a = \sqrt{\omega_a^2 - \omega_e^2}/c$ and $k_b = \sqrt{\omega_b^2 - \omega_e^2}/c$. The cubic nonlinearity [21–23] and group velocity dispersion coefficients are $R = A\omega_e^2\omega_a/4\omega_b^2 V_3$ and $\kappa = AV_3\omega_e^2/[(\omega_b^2 - \omega_e^2)2\omega_b]$. The resonance approximation is valid because the seed bandwidth is within the Raman resonance bandwidth.

The pump is injected at $t = 0$, into, say, the left edge of plasma, $z = 0$. The pump has amplitude $a_0 = 1$ and duration $\Delta_a = L(1 + c_a/c_b)$, so that its front exits the plasma at $z = L$ as the seed enters the plasma, and the rear of the pump enters the plasma at $z = 0$ as the seed exits the plasma. The seed pulse is injected at $z = L$, with a delay, $t = t_d \approx L$, necessary for the pump front to traverse the plasma. The input seed pulse obeys

$$b(L, t) = \frac{b_0 \Delta}{\sqrt{\Delta^2 + 2i\hat{\kappa}z_f}} \exp\left[-\frac{(t - t_d)^2}{2(\Delta^2 + 2i\hat{\kappa}z_f)}\right] \quad (2)$$

with $t_d = L + 3\sqrt{\Delta^2 + 4\hat{\kappa}^2 z_f^2}$, $\hat{\kappa} = \kappa c_a/c_b$, and z_f is the focal length for the linear seed propagation in the absence of pump, under which the seed would reach the shortest duration at $z = L - z_f$, and it is Gaussian in time,

$$b(L - z_f, t) = b_0 \exp\left[-\frac{(t - t_d - z_f c_a/c_b)^2}{2\Delta^2}\right]. \quad (3)$$

For later comparison with theory, it is convenient to characterize the input seed pulse, Eq. (2), not by the amplitude b_0 , but rather by the integrated amplitude, or what we call the *seed capacity*

$$U_{\text{in}} = \frac{2 \int b(L, t) dt}{\sqrt{1 + c_a/c_b}} = U_m \left(1 + \frac{4\hat{\kappa}^2 z_f^2}{\Delta^4}\right)^{1/4}. \quad (4)$$

$$U_m = \frac{2\sqrt{2\pi}b_0\Delta}{\sqrt{1 + c_a/c_b}}. \quad (5)$$

For a given U_{in} , the input seed [Eq. (2)] depends on parameters Δ and z_f , which can be chosen to produce an output pulse of possibly shorter duration and larger intensity.

Assuming that the pump intensity is somewhat below the wave breaking limit with wavelength of $0.351 \mu\text{m}$ and for seed capacity of 0.15, two types of input seed pulses are considered: the nonchirped seed pulse in which $z_f = 0$ and the chirped seed pulse in which $z_f \approx L$. Though theoretically the compression depends on U_{in} , this parameter does not determine uniquely the input seed which depends on two parameters: Δ and b_0 . We choose the parameters Δ and b_0 such that $U_{\text{in}} = 0.15$ and Δ is varied between $0.3t_e$ and $4t_e$, where $t_e = 2\pi AV_3/\omega_e$ is the normalized plasma period. Then to each ω_e/ω_b the result with the shortest output pulse duration was chosen. Figure 1(a) shows the chosen Δ_1 (dashed curve) for chirped seed, Δ_2 (dash-dotted curve) for nonchirped seed, and the plasma length of the chirped seed pulse, L_1 (solid curve). The chirping rate of the seed pulse at $z = L$ is defined as $c_p = (\partial^2 \phi_{\text{in}}/\partial t^2)(1/2\pi)$, where ϕ_{in} is the input seed phase at $z = L$. To inject a chirped seed pulse in the form given in Eq. (2), the required input chirping rate is $c_p = z_f/(2\pi L_d \Delta T^2)$, where the input width of the chirped seed is $\Delta T = \Delta\sqrt{1 + (z_f/L_d)^2}$, and the dispersion length is $L_d = \Delta^2/2\hat{\kappa}$.

That the chirped seed reaches the maximum intensity in a shorter distance can be seen from the solid line in Fig. 1. The point of the maximum intensity is obtained at plasma length $L = L_1$ for chirped seed and $L = L_2$ for nonchirped seed. Figure 1(b) shows the ratio of the plasma length to reach maximum intensity for nonchirped input seed, L_2 , to that for chirped input seed, L_1 . For large ω_e/ω_b , the nonchirped seed takes over twice the distance to reach maximum intensity.

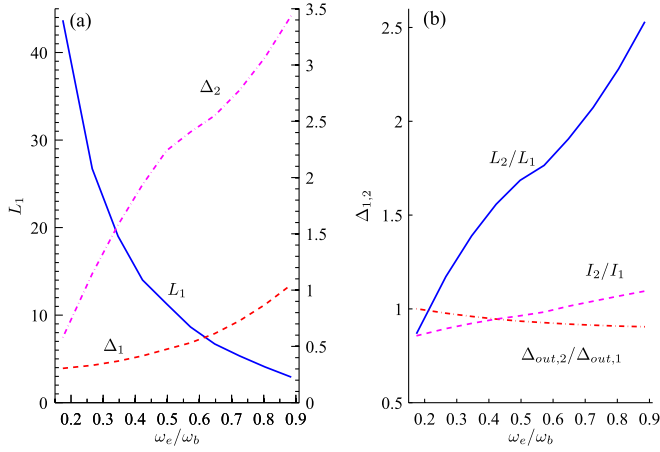


FIG. 1 (color online). (a) The chosen Δ_1 (dashed curve) for chirped seed, Δ_2 (dash-dotted curve) for nonchirped seed, and the plasma length of the chirped seed pulse, L_1 (solid curve) are shown. (b) Comparison of the optimized numerical output parameters for the chirped ($z_f \approx L$) and nonchirped ($z_f = 0$) input pulses as function of ω_e/ω_b with $U_{in} = 0.15$: L_2/L_1 (solid curve); $\Delta_{out,2}/\Delta_{out,1}$ (dash-dotted curve); I_2/I_1 (dashed curve) is shown.

The output pulse reaches the highest intensity in a short spike, followed by several other spikes. The duration of this first spike at its minimum duration is denoted as Δ_{out} . The chirping does not affect the minimum duration or maximum intensity of the first spike, only the length to achieve it. As can be seen from Fig. 1(b), the ratio between the nonchirped and chirped output duration (dash-dotted curve) is approximately unity over a wide range of ω_e/ω_b . Similarly, the dashed curve in Fig. 1(b) shows that the ratio between the nonchirped and chirped output amplified spike intensity is approximately unity over a wide range of ω_e/ω_b . Thus, the output pulse first spike shape is nearly the same for chirped and nonchirped seed pulse at the point of the shortest duration.

In both cases there is nearly complete pump depletion and, by the Manley-Rowe relations, the same fraction of energy goes to the seed pulse. However, because the nonchirped pulse requires twice the length to achieve the same intensity, it also consumes twice the energy. In other words, the chirped seed pulse consumes the same fraction of energy from the pump, but reaches maximum intensity in half the distance. This indicates significant *reshaping* of the output pulse: in the nonchirped seed pulse more energy must go to the later spikes. Thus, to optimize fluence, chirping may not be preferred, but to optimize intensity, it certainly is to be preferred.

To see this reshaping, we show in Fig. 2(a) (solid curve) and Fig. 2(b) (solid curve), at $\omega_e/\omega_b = 0.57$, the normalized output amplitude of the nonchirped and chirped seeds (solid curve) at the point of the shortest duration, respectively. In this example, the plasma length for the chirped seed is $L_1 = 8.63$ and for the nonchirped seed is $L_2 = 16.7$,

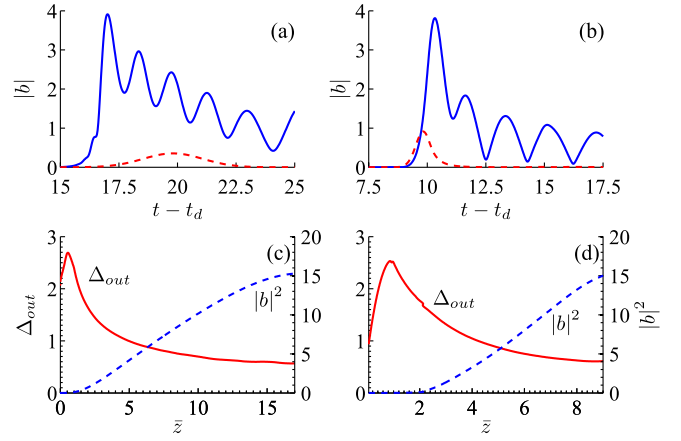


FIG. 2 (color online). Pulse evolution comparison between the nonchirped seed and the chirped seed pulse at $\omega_e/\omega_b = 0.57$. (a) and (b): Output amplitude of the seed pulse (solid curves) for input nonchirped and chirped seed pulses at point of shortest duration, respectively; corresponding seed profiles (dashed curves) when the pump pulse is absent are scaled up by a factor of 10 to be visible. (c) and (d) show the seed width (solid curves) for nonchirped (c) and chirped (d) seed pulses; dashed curves, corresponding square amplitudes of the first spike, $|b|^2$. Here, \bar{z} is the distance propagated by the seed (with respect to the right edge of the plasma).

which is about twice the distance traversed by the chirped seed. In both cases, the first spike is approximately the same both in peak intensity and in width. However, higher levels of side lobes appear in Fig. 2(a) than in Fig. 2(b), which means that the total output fluence of the nonchirped seed is larger than the chirped seed.

Also, in both cases, the fraction of energy that goes from the pump to the seed is approximately 50% because the pump depletion is not quite complete. This value is close to the Manley-Rowe theoretical limit of $\omega_b/\omega_a \approx 64\%$. The first spike has the same energy in both cases, but the rest of the nonchirped seed energy is 37% of the input pump energy (while for the chirped seed pulse it is 20%), indicative of the reshaping.

Figures 2(a) and 2(b) show also the seed pulse profiles (dashed curves) when the pump pulse is absent. Both seed pulses, in the absence of the pump (dashed curves), propagate the same distance as the corresponding amplified seed pulses (solid curves). A comparison of the seed pulses in the absence of the pump (dashed curves) with the seed pulses in the presence of the pump (solid lines) can explain why seed chirping enables BRA at shorter plasma lengths. At the first stage of the BRA (known as the linear regime) the pump pulse is almost constant. The seed pulse comprises two pulses: the original seed pulse in front, and, in the trailing edge, the amplified pulse. The original seed in front is actually like the seed pulse in the absence of the pump. Later, when the pump is significantly depleted, the leading, major spike of the amplified pulse contracts. While the original seed propagates at group velocity

smaller than the speed of light, the leading spike of the amplified pulse propagates at a superluminal velocity, thus narrowing the gap between the spike and the original seed. The full amplification potential of the seed pulse is realized when most of the original seed stays within that gap throughout the entire BRA process. This requirement, relatively mild in strongly undercritical plasmas, turns out to be more challenging in moderately undercritical plasmas, where larger group velocity dispersion tends to stretch more quickly the short seed pulses.

Because the chirped seed pulse reaches its minimum duration close to the exit of the plasma, most of the self contracted seed can stay in front of the major amplified spike, as seen clearly in Fig. 2(b). On the other hand, contraction reduces the integrated seed amplitude, thus reducing the seed amplification potential. However, this reduction may be less than what occurs when the major amplified spike encroaches upon and shadows the seed, as can be seen in Fig. 2(a) for the nonchirped seed pulse.

Figures 2(c) and 2(d) show the full width at half maximum (FWHM) of the nonchirped and chirped seed pulses (solid curves) and its normalized intensity (dashed curves), $|b|^2$, respectively. As seen from Figs. 2(c) and 2(d) the output shortest duration in both cases is $\Delta_{\text{out},1} \approx \Delta_{\text{out},2} \approx 0.6$ with maximum squared amplitude of 15.

For the example shown in Fig. 2 with $0.351 \mu\text{m}$ pump wavelength (like lasers used in National Ignition Facility [30]) the electron density is $n_e = 12 \times 10^{20} \text{ cm}^{-3}$. The input pump intensity is 121.8 PW/cm^2 . For the chirped seed case the input seed intensity is 0.27 PW/cm^2 , input FWHM of 4.4 fsec , and $z_f = 12 \mu\text{m}$. Here, the input chirp rate of the chirped seed is 20 THz/fsec . The seed input bandwidth is $0.2f_b$, where $f_b = \omega_b/2\pi = 544 \text{ THz}$. Also, the plasma length is $L_1 = 16 \mu\text{m}$, which corresponds to 0.11 psec pump width. For the nonchirped seed case the input seed intensity is 0.09 PW/cm^2 , input FWHM of 12 fsec . In the nonchirped seed case the plasma length is $L_2 = 31 \mu\text{m}$, which corresponds to 0.22 psec pump width. The seed input bandwidth is $0.04f_b$. In both chirped and nonchirped seed cases that output intensity is 1.15 EW/cm^2 with FWHM of 3.2 fsec . Hence, the output fluence is 3.68 kJ/cm^2 .

It was reported that particle-in-cell simulations with nonchirped seed pulse showed that the optimal regime of BRA lies in the range of $10 \leq \omega_a/\omega_e \leq 14$, where the scanned domain was $10 \leq \omega_a/\omega_e \leq 40$ [24,25]. For smaller laser-to-plasma frequency ratio, other deleterious effects such as transverse filamentation and forward Raman amplification can limit the efficiency of the BRA [24]. But forward Raman amplification is significantly smaller when the pump is chirped and the density has a gradient [26]. And the transverse filamentation needs the same or more time to develop than the longitudinal one which was considered here as the relativistic effect [2].

Here, however, we scanned the range of $0.2 \leq \omega_e/\omega_b \leq 0.9$ (or $2.13 \leq \omega_a/\omega_e \leq 6.7$) where larger laser

pulses intensities can be achieved. High intensity laser pulses can be produced by chirped seeds at significantly shorter length than nonchirped seed pulse. The short plasma length for chirped seed pulse is advantageous as other deleterious effects such as inverse bremsstrahlung [27,28], forward Raman amplification, and filamentation [29] have less time to reduce the efficiency of the BRA. Also, less plasma length means less input pump energy is required to obtain high output intensity.

To summarize, seed chirping can produce higher intensity laser pulses over shorter plasma lengths. The largest length ratio occurred at high density where the group velocity dispersion of the seed pulse becomes a dominant effect. Shortening the plasma length at high plasma densities preserves the input seed capacity as most of the original seed pulse stays in front of the major amplified spike. The seed pulse is chirped such that its minimum duration, when the pump is absent, would occur at the plasma exit.

Both chirped and nonchirped seeds consume the same fraction of pump energy. Hence, the ratio between their total output fluences is simply the ratio of the plasma lengths utilized. However, the seed pulse can be differently shaped. Higher output total fluence can be produced for the nonchirped seed such that the first spike has the same fluence. But the same intensity can be reached in half of the length by chirping the seed. This means that with different seed chirping one can control the amount of the total output fluence such that the first spike fluence remains constant.

Although BRA is desirable for achieving the next generation of laser intensities, it is not desirable in inertial confinement fusion [30]. However, techniques such as chirping introduced here to optimize the amplification might also find use in reducing amplification when it is not wanted.

This work was supported through the NNSA SSAA Program through DOE Research Grant No. DE274-FG52-08NA28553 and U.S. DTRA.

-
- [1] D. Strickland and G. Mourou, *Opt. Commun.* **56**, 219 (1985).
 - [2] V.M. Malkin, G. Shvets, and N.J. Fisch, *Phys. Rev. Lett.* **82**, 4448 (1999).
 - [3] D.S. Clark and N.J. Fisch, *Phys. Plasmas* **10**, 3363 (2003).
 - [4] R. K. Kirkwood *et al.*, *J. Plasma Phys.* **77**, 521 (2010).
 - [5] V.M. Malkin, G. Shvets, and N.J. Fisch, *Phys. Plasmas* **7**, 2232 (2000).
 - [6] N.J. Fisch and V.M. Malkin, *Phys. Plasmas* **10**, 2056 (2003).
 - [7] N. A. Yampolsky, N. J. Fisch, V. M. Malkin, E. J. Valeo, R. Lindberg, J. Wurtele, J. Ren, S. Li, A. Morozov, and S. Suckewer, *Phys. Plasmas* **15**, 113104 (2008).

- [8] Y. Ping, W. Cheng, S. Suckewer, D.S. Clark, and N.J. Fisch, *Phys. Rev. Lett.* **92**, 175007 (2004).
- [9] C.H. Pai, M.-W. Lin, L.-C. Ha, S.-T. Huang, Y.-C. Tsou, H.-H. Chu, J.-Y. Lin, J. Wang, and S.-Y. Chen, *Phys. Rev. Lett.* **101**, 065005 (2008).
- [10] Y. Ping *et al.*, *Phys. Plasmas* **16**, 123113 (2009).
- [11] T.L. Wang, D.S. Clark, D.J. Strozzi, S.C. Wilks, S.F. Martins, and R.K. Kirkwood, *Phys. Plasmas* **17**, 023109 (2010).
- [12] G. Vieux *et al.*, *New J. Phys.* **13**, 063042 (2011).
- [13] X. Yang, G. Vieux, E. Brunetti, J.P. Farmer, B. Ersfeld, S.M. Wiggins, R.C. Issac, G.H. Welsh, and D.A. Jaroszynski, *Proc. SPIE Int. Soc. Opt. Eng.* **8075**, 80750G (2011).
- [14] G.A. Mourou, N.J. Fisch, V.M. Malkin, Z. Toroker, E.A. Khazanov, A.M. Sergeev, T. Tajima, and B. Le Garrec, *Opt. Commun.* **285**, 720 (2012).
- [15] N.A. Yampolsky, V.M. Malkin, and N.J. Fisch, *Phys. Rev. E* **69**, 036401 (2004).
- [16] V.M. Malkin and N.J. Fisch, *Phys. Plasmas* **12**, 044507 (2005).
- [17] V.M. Malkin, Z. Toroker, and N.J. Fisch, *Phys. Plasmas* **19**, 023109 (2012).
- [18] V.M. Malkin, N.J. Fisch, and J.S. Wurtele, *Phys. Rev. E* **75**, 026404 (2007).
- [19] V.M. Malkin and N.J. Fisch, *Phys. Rev. E* **80**, 046409 (2009).
- [20] V.M. Malkin and N.J. Fisch, *Phys. Rev. Lett.* **99**, 205001 (2007).
- [21] A.G. Litvak, *Zh. Eksp. Teor. Fiz.* **57**, 629 (1969) [*Sov. Phys. JETP* **30**, 344 (1970)].
- [22] C. Max, J. Arons, and A.B. Langdon, *Phys. Rev. Lett.* **33**, 209 (1974).
- [23] G.-Z. Sun, E. Ott, Y.C. Lee, and P. Guzdar, *Phys. Fluids* **30**, 526 (1987).
- [24] R.M.G.M. Trines, F. Fiúza, R. Bingham, R.A. Fonseca, L.O. Silva, R.A. Cairns, and P.A. Norreys, *Nature Phys.* **7**, 87 (2010).
- [25] R.M.G.M. Trines, F. Fiúza, R. Bingham, R.A. Fonseca, L.O. Silva, R.A. Cairns, and P.A. Norreys, *Phys. Rev. Lett.* **107**, 105002 (2011).
- [26] V.M. Malkin, G. Shvets, and N.J. Fisch, *Phys. Rev. Lett.* **84**, 1208 (2000).
- [27] V.M. Malkin and N.J. Fisch, *Phys. Plasmas* **17**, 073109 (2010).
- [28] A.A. Balakin, N.J. Fisch, G.M. Fraiman, V.M. Malkin, and Z. Toroker, *Phys. Plasmas* **18**, 102311 (2011).
- [29] G.M. Fraiman, N.A. Yampolsky, V.M. Malkin, and N.J. Fisch, *Phys. Plasmas* **9**, 3617 (2002).
- [30] J.D. Moody *et al.*, *Nature Phys.* **8**, 344 (2012).